

Reinterpretation of the scanning tunneling microscopy images of Si(100)-(2×1) dimers

Kenji Hata,* Satoshi Yasuda, and Hidemi Shigekawa*

Institute of Applied Physics and CREST, Japan Science and Technology Corporation (JST), University of Tsukuba, Tennodai 1-1-1, Tsukuba 305-8573, Japan

(Received 4 May 1998; revised manuscript received 1 April 1999)

We revisit and refine the interpretation of the scanning tunneling microscopy (STM) images of the Si(100) dimers, based on results from an extensive set of STM observations carried out at low temperature (80 K) and total-energy calculations of Si(100) surfaces. The interpretation addresses some unresolved questions and brings much experimental and theoretical research into unanimous agreement. We show that tunneling from surface resonances and bulk states seriously contributes to the STM images within usual tunneling conditions. In the empty state, tunneling from these states overwhelms tunneling from the localized π^* surface state, which STM is generally believed to observe. [S0163-1829(99)05935-4]

I. INTRODUCTION

Even though the dimer of Si(100) is one of the most simple surface reconstructions, it has turned out to be a source of never-ending controversy. A great deal of research has been devoted to elucidate its atomic configuration, optical properties, and electronic structure.¹⁻⁶ In particular, scanning tunneling microscopy (STM) has considerably contributed to enlighten our understandings.¹⁻⁶ Generally, it is interpreted that STM observes the surface states localized at the dangling bonds of the dimers.^{1,2} Interpretation of the STM images of the dimers from this standpoint seems to be simple and in accordance with what is expected from the general laws of chemical bonding.¹ However a careful analysis of the existing data reveals that our understanding is not complete, and in the following we point out two problems which require further consideration.

The first question is concerned with the interpretation of the filled-state STM images obtained at room temperature up to now. Previous room-temperature STM studies show dimers as bean-shaped protrusions which have a maximum at the center of the Si-Si dimer bond in the filled states.^{1,2} We nominate them as bean-type dimers in the following. In contrast, when the empty states are probed, two round shape protrusions are resolved,² which we refer to as protrusion-type dimers. These STM images are easily explained by assuming symmetric dimers,¹ though it is now well established that dimers are buckled.³ Indeed at temperatures below ~ 200 K (low temperatures), a majority of the dimers is observed in a buckled configuration.³ Buckling induces a charge transfer from the lower to upper atom of the dimer, and the filled π and empty π^* surface states are localized at the dangling bonds of the upper and lower atoms of the buckled dimer, respectively. Generally, it is assumed that the π and π^* surface states^{1,2} are observed in the STM images as dimers. In order to interpret the apparent symmetric dimers observed by STM at room temperature within the framework of buckled dimers, the concept of flip-flop motion was introduced: buckled dimers are flip-flopping far faster than the scanning of STM, thus dimers appear in an apparent symmetric configuration. In this scheme, STM images obtained at room temperature must reflect the average of STM images of the buck-

led dimers at low temperature in the two possible configurations. It is easy to interpret the empty-state images at room temperature: the two protrusions observed in the (2×1) unit cell are both the π^* surface state localized at the lower atom of the buckled dimer in the two possible configurations. On the other hand, it is puzzling why similar protrusion-type dimers are not observed in the filled state instead of the bean-shaped dimers. Indeed, in Fig. 1 we show gray scale images of the simulated spatial distribution of the flip-flopped filled π and empty π^* surface states calculated by first-principle methods. Methodology of the first-principle calculations is presented in Sec. III C. Flip-flop motion was simulated by adding the electronic structure of the surface states in the two possible configurations of the buckled dimer. It is a surprise to notice that the images of the flip-flopped π and π^* surface states are very similar with a small node in between the dimer. A similar result has been obtained by Owen *et al.*, where they simulated STM images of the flip-flopping buckled dimers following Tersoff and Hamman's formalism. Their simulation shows a protrusion-type STM image of the dimers in the filled states [Fig. 2(a) in Ref. 7].

The second problem is the mismatch between the typical surface bias used to observe the surface in the past and the energy window where the π and π^* surface states are localized. A survey of previous STM observations of the Si(100)

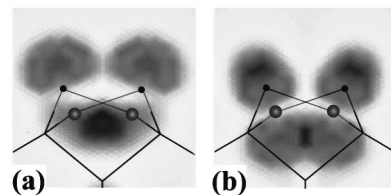


FIG. 1. Cross sections of the electronic and atomic structure of the simulated flip-flopped buckled dimers. (a) Simulated filled π surface state and (b) π^* empty surface state. Cross sections were taken along a plane which includes the buckled dimer. The small black and large gray circles represent the position of the upper and lower atom of the buckled dimer, respectively. The electronic structure was calculated by first-principles methods and the flip-flop motion was simulated by adding the two possible configurations.

surface reveals that most of the STM images are of the filled states taken with a surface bias as large as -2 V.¹⁻⁵ However, the typical bias of -2 V is out of the range of where the π surface state is located. We can see this by considering the surface band gap and the width of the surface states. Typical I - V curves of the dimers show a surface band gap of ~ 0.5 V with the Fermi level located in the midgap.⁴ The surface band gap of ~ 0.5 V is also supported from other experiments.⁸ Theoretical⁹ and photoemission^{10,11} studies show that the bandwidths of the π and π^* states are 0.6 – 0.8 V each. When combined with the surface band gap of ~ 0.5 V, this means that the π and π^* surface states are roughly localized in the range of ± 1 V from the Fermi level. In a typical STM image taken at -2 V, a significant part of the tunneling current must come from states other than the surface π and π^* states.

In this paper, we provide results from an extensive set of STM observations at room and low temperature (80 K), and present a refined interpretation of the STM images of dimers. In our interpretation, at typical tunneling conditions used in the past, a serious part of the tunneling current comes from states other than the π and π^* surface states. The new interpretation addresses the aforementioned unresolved questions and brings results of much experimental and theoretical research into unanimous agreement.

II. EXPERIMENT

Defects are the major reason why high biases (~ -2 V) were used in the past. It is believed that surfaces of Si(001) inevitably contain a significant density of defects. When one attempts to lower the bias, these defects become very bright because many defects are metallic, making it difficult to observe the dimers clearly. We have overcome this problem by fabricating a surface with very low defect density. After the sample was prebaked at ~ 700 °C for one night, it was flashed to 1200 °C for several seconds. The pressure was kept below 1×10^{-8} Pa during flashing (in most times around 5×10^{-9} Pa). We found that keeping this extremely good vacuum pressure during flashing is crucial to have a surface with low defect density.¹² By this procedure, a clean Si(100) surface with a small ratio of defects lower than 0.2% was repeatedly made on any provided sample. N -type Si samples phosphorus-doped with a conductivity of 0.1 Ω cm were used. Tunneling I - V measurements of the surface show that the Fermi level is at the upper edge of the conduction band, which agrees with the n -type doping, and a width of the surface band gap was ~ 0.5 V.

III. RESULTS AND DISCUSSION

A. STM results at room temperature

Surfaces free from defects make observation of the dimers possible at any desired surface bias. Figure 2(a) shows an STM image of the filled state probed with a low surface bias just below the surface band gap (-0.6 V) at room temperature. Not a bean-type but a protrusion-type dimer is observed. We could observe the protrusion-type dimers in the filled states at low surface biases with the same frequency as in the empty state. The protrusions are observed at the same location where the empty-state protrusions are observed, thus

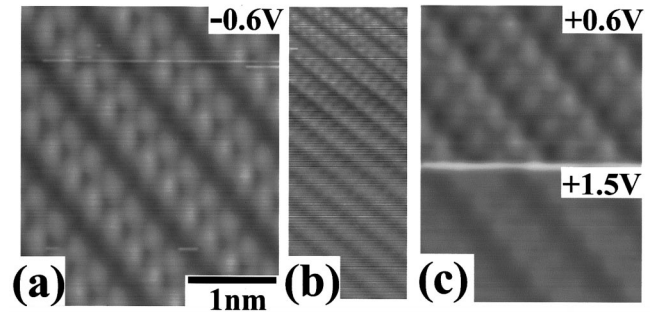


FIG. 2. STM images of dimers at room temperature. (a) Low bias filled state (-0.6 V). (b) The bias was gradually decreased from -0.9 to -1.7 V. The bean \leftrightarrow protrusion transition of the dimers occurred around ~ -1 V. The reason why the bean-shaped dimers are not clearly visible at high biases might be because this image was taken simultaneously with the protrusion-type dimers observed at low biases, which show stronger contrast than the bean-type dimers. (c) Empty-state image. The surface bias was switched from a low ($+0.6$ V) to a high ($+1.5$ V) bias in the middle.

we attribute them to be observing the π surface state located at the dangling bond of the upper atom of the dimer. Every time the bias is increased, the dimers would gradually revert to the bean type at ~ -1 V as shown in Fig. 2(b), in a reversible fashion. This indicates that the protrusion-type dimers observed here are not induced by some peculiar tip-surface interaction.

The empty-state STM images show a more complicated dependence on bias. When the surface bias is above $+1.4$ V, regions between the dimer rows are observed. This is highlighted in Fig. 2(c), where the bias was switched from a low (0.6 V) to a high bias (1.5 V) in the intermediate of scanning. Immediately it is apparent that the bright rows observed at low (0.6 V) and high biases (1.5 V) are completely out of phase. We attribute the bright rows observed at low biases to the dimers, since they are in-phase with the dimer rows observed in the filled state. This means that regions between the dimers are observed at high biases. The phase shift occurs at a bias around 1.4 V. The phase shift was reported previously¹ and was interpreted as an extension of the node of the antibonding state of a symmetric dimer with bias which was lately supported by theoretical studies.¹³ However, as mentioned before, dimers are buckled, and the π^* surface state of buckled dimers is calculated not to show such an extension with bias.¹³ Considering these points, we interpret that at high biases, the main part of the tunneling current comes from states localized between the dimer rows, overwhelming tunneling from the π^* surface state.

Results obtained at room temperature are summarized. Protrusion-type dimers are observed both in the empty and filled states at low biases. On the other hand, at high biases, bean-type dimers are observed in the filled states while the region between the dimer rows is observed in the empty states. We interpret the results as the following. (i) At low biases, STM observes the π or π^* surface states. The protrusion-type dimers are observed as a result of the flip-flop motion of the buckled dimers. The range of surface biases (-1 V to $\sim +1.4$ V) where the protrusion-type dimers is observed is in good accordance with the energy window where the π and π^* bands are localized. (ii) At high biases,

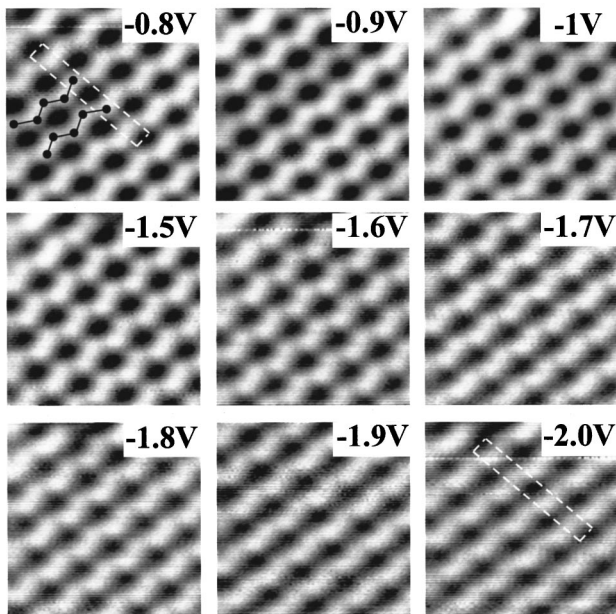


FIG. 3. STM images (1 nA) of the filled states of the dimers at surface biases ranging from -0.8 to -2.0 V at 80 K. Scale 4×4 nm.

tunneling from other states starts to participate in, and in the empty states overwhelm, tunneling from the π^* surface state. The spatial distribution of the other states is localized between the Si-Si dimer bond in the filled states and between the dimer rows in the empty states, respectively. The new STM images and interpretation presented here address the two problems mentioned in the Introduction. Moreover, many experimental results—the widths of the π and π^* bands, surface band gap obtained from I - V curves, and the voltage dependence of the STM images—come into solid coincidence within the familiar notion of flip-flopping buckled dimers.

B. STM results at low temperature (80 K)

In order to reinforce our assertions, an extensive set of STM observations was carried out at a low temperature (80 K) where the flip-flop motion of dimers is frozen. We show that the low-temperature STM images of the dimers unanimously coincide with the complementary room-temperature results further supporting our interpretation.

First we provide results of the observation of the filled states. Figure 3 shows some typical filled-state STM images of the dimers with different biases ranging from -0.8 to -2.0 V to show the dependence of the STM images on surface bias. STM images taken at low bias (~ -1.0 V) show clear zigzag chains forming a $c(4 \times 2)$ phase,³ which we interpret to reflect tunneling from the π surface state localized at the upper atom of the dimer. The upper atom of the dimers and the dimer rows are aligned in an antiferromagnetic order providing the observed $c(4 \times 2)$ phase. Based on this understanding, the locations of the upper atoms of the dimers are assigned as black circles in the STM image taken at -0.8 V. As the bias is increased, the $c(4 \times 2)$ zigzag component fades and instead a (2×1) component emerges and grows in intensity as shown in the STM images taken at

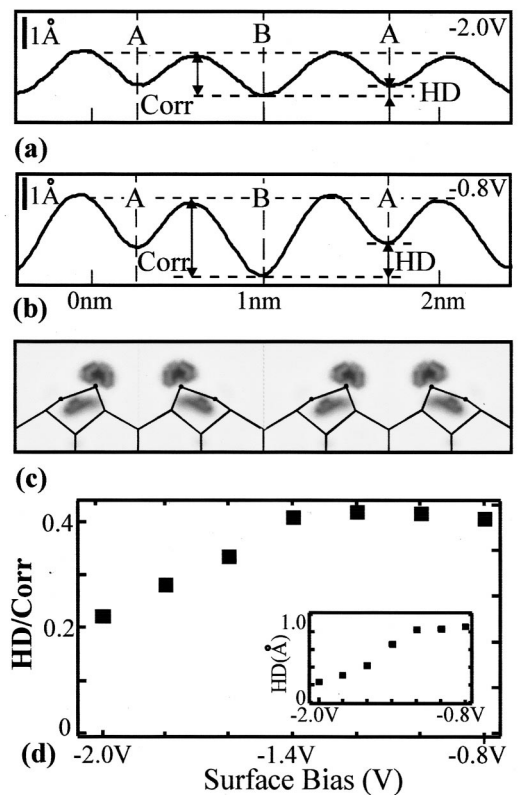


FIG. 4. Average cross section of the filled-state STM images taken at (a) a high bias (-2.0 V) and (b) a low bias (-0.8 V). (c) Cross section of the electronic structure of the filled π surface state. Two types of minima indicated by A and B in the cross sections exist aligned alternatively. HD is defined as the height difference between A and B, and Corr as the average corrugation of the dimers. (d) Dependence of HD/Corr on surface bias. Also HD vs surface bias is displayed in the inset.

high biases above -1.5 V. At -2 V, the STM image resembles a $c(4 \times 2)$ zigzag component overlapped with a (2×1) component. In order to investigate this fading effect more quantitatively, average cross sections of the dimers in the STM images taken at high (-2.0 V) and low (-0.8 V) biases are shown in Figs. 4(a) and 4(b), respectively. Cross sections are taken at the locations displayed as dashed boxes in Fig. 3. In addition, we display the cross section of the electronic structure of the π surface state calculated by first-principle methods in Fig. 4(c) for comparison. We registered Fig. 4(c) against Figs. 4(a) and 4(b) by attributing the global minimum of the cross sections to the middle of the dimer rows where the lower atoms of the dimers are at the adjacent. By comparing Figs. 4(b) and 4(c), we can understand that STM is not observing the atoms of the dimers and the corrugation in the STM images reflects the global corrugation of the electronic structure with some diminished spatial resolution. From Fig. 4(b), it is apparent that there exists two types of minima aligned alternatively in the cross sections. Minima A and B defined in Fig. 4 are both located in the middle between the dimers, though they are different because the upper (lower) atoms are located at the immediate adjacent of minimum A (B). This difference is due to the $\times 4$ periodicity of the reconstruction in this direction and gradually decreases as the bias is increased as shown in Fig. 4(a). We define the height difference between the two minima A and B

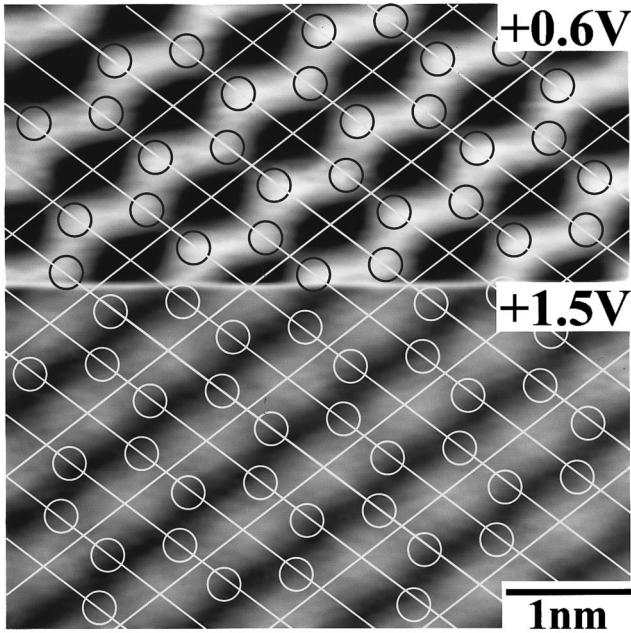


FIG. 5. An STM image (1 nA) of the empty states at 80 K. (a) The bias was switched from a low (0.6 V) to a high (1.5 V) bias in the middle.

as HD, and the average corrugation of the dimers as Corr as shown in Figs. 4(a) and 4(b). HD divided by the corrugation of the dimers (Corr) is assumed to serve as an indicator of the strength of the $c(4 \times 2)$ zigzag component versus the (2×1) component. The dependence of HD/Corr on the surface bias is plotted in Fig. 4(d). Also HD versus surface bias is displayed in the inset of Fig. 4(d). HD/Corr remains constant below -1.4 V and gradually decreases with increased biases. It should be noted that even at biases as high as -2 V, HD/Corr does not drop to zero, thus the remaining $c(4 \times 2)$ zigzag component should have been observed and reported as buckled dimers in previous studies.^{3,14-16} We interpret the experimental results as the following. (i) Tunneling from the π surface state is observed at low biases near the Fermi edge. (ii) A decrease of the $c(4 \times 2)$ zigzag component at high bias reflects an opening of a new tunneling channel from other states which are mainly localized in between the Si-Si dimer bond and have an almost (2×1) periodicity. (iii) As the bias is increased, tunneling from other states becomes important and the $c(4 \times 2)$ zigzag component fades. Tunneling from the other states at high biases should be the cause of the protrusion \leftrightarrow bean-type transitions of the appearance of the dimers observed in the filled states at room temperature.

Next, we shift to the observations of the empty states at low temperature. Figure 5 shows an STM image at low temperature (80 K) where the bias was switched from a low (0.6 V) to a high bias (1.5 V) in the intermediate. Again, the phase shift is observed, and areas between the dimer rows are observed at the high bias. Dimers appear different in the STM images taken at low and high biases. At the low bias, STM images show rows of zigzag chains in a $c(4 \times 2)$ phase,³ which reflects tunneling from the π^* surface state localized at the lower atom of the dimer. In contrast, at the high bias, a bright row similar to that observed at room temperature is obtained, though a bright and dark (2×1) unit

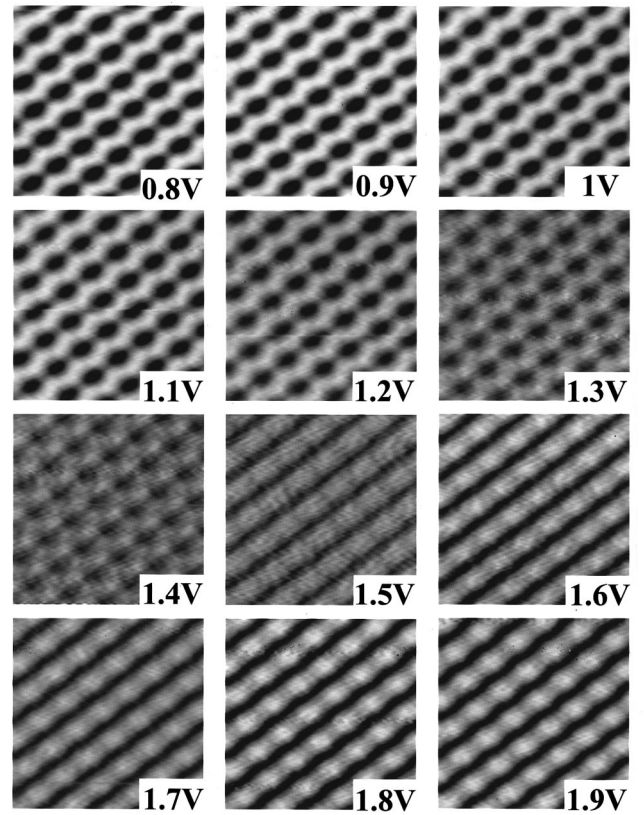


FIG. 6. STM images of the empty states at surface biases ranging from 0.8 to 1.9 V at 80 K. Tunneling current 0.6 nA. Scale 5×5 nm.

align alternatively along the dimer-row direction. The brighter units are registered against the $c(4 \times 2)$ region scanned with low bias, from which we attribute the lower atom of the dimer to a circle as shown in Fig. 5. It shows that the brighter unit corresponds to the location of the upper atom of the dimer. This cannot be explained by an extension of the wave function of the π^* state localized at the lower atom with bias, but means that tunneling from other states becomes important at high biases. In order to investigate the details of the phase shift with bias, we have carried out STM observations of the dimers on a defect-free $c(4 \times 2)$ buckled dimer domain scanned with different biases ranging from 0.8 to 2.1 V with an increase rate of 0.1 V as shown in Fig. 6. Also a set of cross sections of the STM images of Fig. 6 along the dimers are displayed in Fig. 7. In the lower section of Fig. 7, the cross section of the calculated electronic structure of the π^* surface state is displayed for clarity. Registry was done in the same fashion employed to display Fig. 4(c). The same phase shift presented in Fig. 5 is evident. At low biases below 1.4 V, two types of minima in the cross sections are clearly observable, which reflects the $c(4 \times 2)$ zigzag component, likewise the case of the observations of the filled states. We interpret that tunneling from the π^* surface state localized at the lower atom of the dimer is observed at these low biases. As the bias increases and approaches 1.4 V, the corrugations of the dimers gradually decrease, which should reflect an opening of tunneling channels from other states. It is a surprise to observe an almost flat STM image at the transition bias of 1.4 V. As the bias is increased above

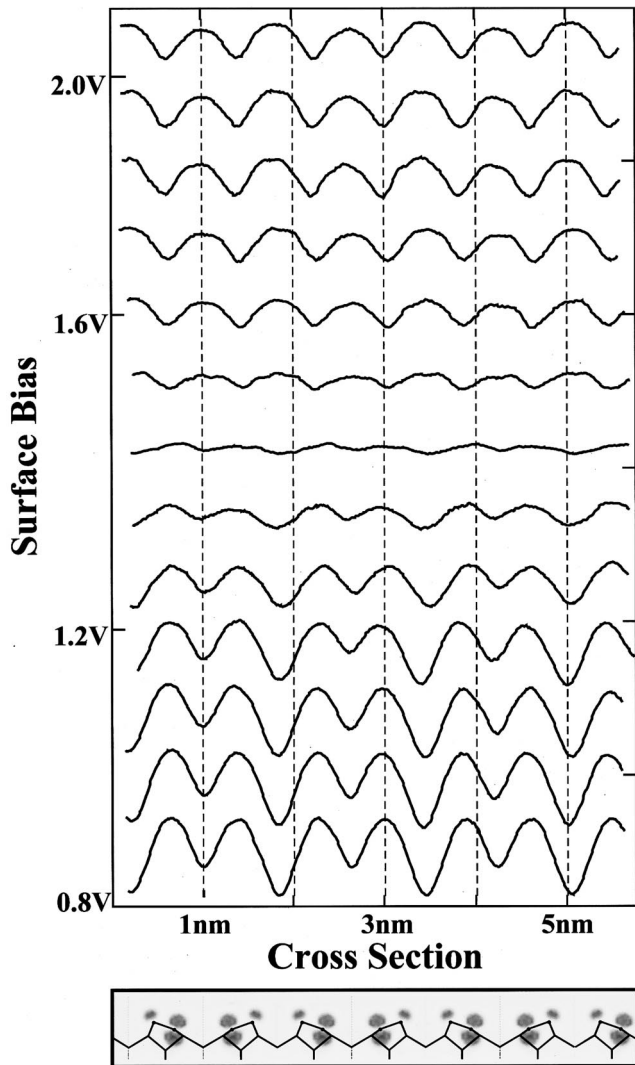


FIG. 7. Cross section of STM images of Fig. 6 along the dimers. The inset in the bottom shows the cross section of the electronic structure of the π^* surface state.

1.4 V, a new corrugation emerges which is out of phase with that observed at low biases. The new corrugation observed at high biases is characterized by two types of maxima aligned alternatively forming a $\times 4$ periodicity in contrast to the two types of minima observed at low biases. Again, the low-temperature results are fully consistent with the room-temperature observations.

Subsequently, we register the filled-state STM images against the empty-state images taken at low biases to emphasize their similarity and to show that band bending does not affect our interpretation. Figure 8 shows an STM image of the dimers at low temperature (80 K) where the bias was switched from positive to negative in the intermediate of scanning at the location indicated by the black line. Hence, the upper half is an empty-state image while the lower half is an image of the filled state both taken at low biases. Similarity between the dimers in the STM images of the empty and filled states is striking, which agrees with the protrusion-type image of dimers obtained at room temperature both in the empty and filled states at low biases. Moreover, what is more important is that the opposite side of the dimer is ob-

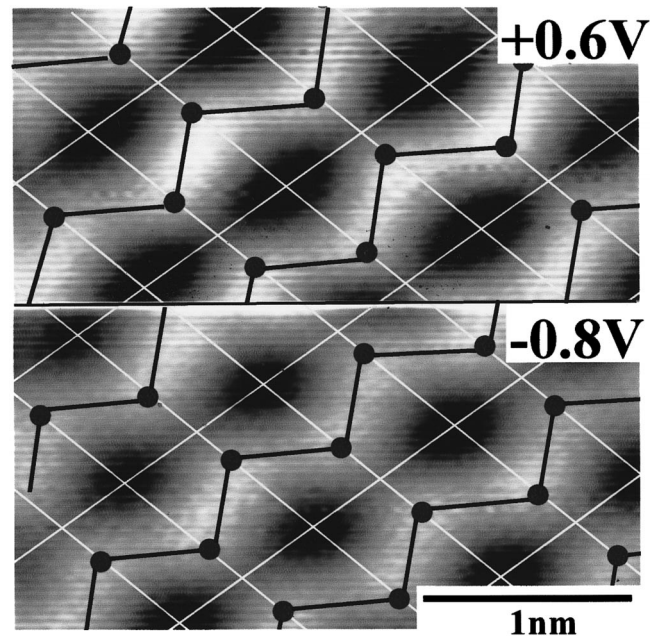


FIG. 8. An STM image (1 nA) showing both the filled and empty states at 80 K. The bias was switched from positive (+0.6 V) to negative (-0.8 V) in the intermediate of scanning at the location of the black line. The stick and ball schematics are assigned to the $c(4 \times 2)$ zigzag components of the STM image, which reflect tunneling from the π^* and π surface states.

served in the empty and filled states. This is emphasized by matching a $c(4 \times 2)$ phased stick and ball pattern to the $c(4 \times 2)$ zigzag component of the STM image. Obviously the stick and ball patterns observed in the empty and filled states are out of phase, giving other evidence that the π and π^* surface states localized at the opposite side of the dimer are observed in the STM images taken at low biases. Fur-

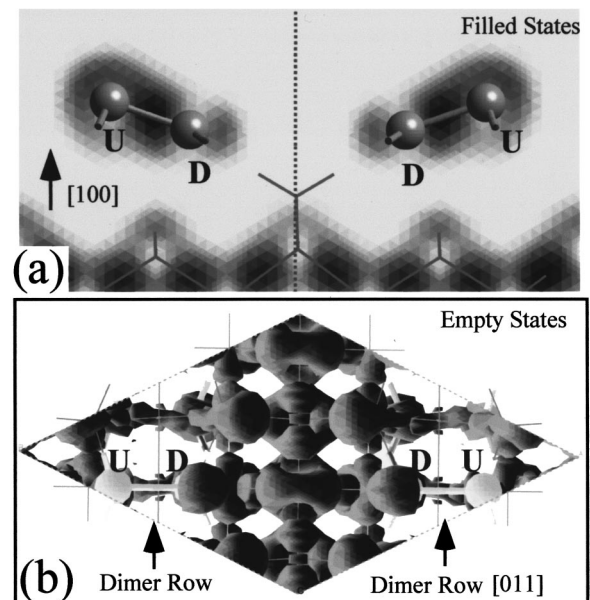


FIG. 9. Spatial distribution of the electronic density of states of the buckled dimers within ± 2 V of the Fermi energy except the π and π^* bands. (a) Filled states. (b) Empty states. D and U indicate the lower and upper atoms of the buckled dimer, respectively.

thermore, we can definitely state that the filled-state STM images taken at low bias are really observing the filled states, not the empty states. This is important because it excludes the possibility that the appearance of protrusion dimers observed at room temperature in the filled states at low biases is due to observing the empty states at negative surface bias as a result of band bending.

Variation of the tip-surface distance with bias is another possible explanation for the dependence of the STM images on bias. All of the STM images in Figs. 3 and 6 were taken at a constant current, thus an increase in bias means an increase in the tunneling barrier height and the tip-surface distance. Generally, an increase in the tip-surface distance results in a decrease of resolution, which one might suspect to be the cause of the protrusion \leftrightarrow bean (room-temperature), zigzag \leftrightarrow bean transitions (low temperature) of the appearance of the dimers observed in the filled states. However, by this mechanism the phase shift observed in the empty states cannot be explained. Furthermore, STM images taken at constant barrier height ($1 \times 10^9 \Omega$) also show an identical transition shown in Figs. 3 and 6 at the same bias in the same fashion. Strictly speaking, constant barrier height does not mean a constant tip-surface distance. Since the feedback of STM is regulated to keep the tunneling current constant at a particular bias, it is difficult to scan the surface with the same tip-surface distance at different biases. Considering these factors, we have compared STM images taken with a large barrier height (far from the surface) at low biases (-1 V, 100 pA) and with a small barrier height (close to the surface) at high biases (-2 V, 64 nA). The STM images were basically the same, though somewhat of an increase of the zigzagged chain component was observed at high bias. We did not observe complete zigzag chained dimers at high biases, thus we rule out the variation of tip-surface distance as the main cause of the dependence of STM images on bias.

C. Theoretical calculations

STM observations consistently show that tunneling from states other than the π and π^* surface states becomes important at high biases. In this section we briefly discuss the possible states observed at high biases. As the π and π^* are the only localized surface states of the buckled dimers, we have to consider the more extended surface resonances and the bulk continuum states. We refer to the calculations carried out by Kruger *et al.*,^{17,18} where they have employed a self-scattering theoretical method based on first principles which is suited to calculate surface resonances extending a long range into the bulk. In their calculations, the back bond (B_1) and dimer bond (D_1, D_i^*) states were shown to lie close to the π and π^* surface states in energy (look at Fig. 5 in Ref. 18). We assign them as the states observed by STM at high voltages.

In order to give a rough idea of the spatial distributions of these states, the spatial distribution of overlapped bands within ± 2 V of the Fermi energy in the filled and empty states, except the π and π^* bands, was calculated. Standard formalism of first-principle calculations was employed with the local-density approximation and plane-wave-based non-local pseudopotentials with a cutoff energy of 10 Ry. Calculations were carried out on a $c(4 \times 2)$ supercell containing a slab of silicon ten layers thick geometrically optimized by Ramstad⁹ with a vacuum region of five layers thickness. It must be noted that the supercell technique is not suited to treat surface resonances which extend into the bulk. Hence, in this paper, the aim of our calculation is to roughly estimate whether or not the spatial distribution of bands located near to the Fermi energy, except the π and π^* bands, is similar to what was observed in the STM images at high biases. Figure 9 shows the spatial distribution of states near the Fermi energy except the π and π^* bands. A strong intensity in the middle of the Si-Si dimer bond in the filled states [Fig. 9(a)] is observed, while they are localized mainly between the dimer rows in the empty states [Fig. 9(b)], in coincidence with the STM observations. In order to give a more detailed analysis, we have to calculate the surface resonances with a more proper method or use a very deep cell in which the effect of the thickness of the cell becomes negligible. Also we have to simulate the STM images by combining the calculated electronic structures with the tunneling probabilities. Matching STM images and theoretical calculations would be an interesting subject for future work.

IV. CONCLUSIONS

This study has two important implications for future STM studies on Si(100). First, careful attention must be paid when one observes the empty states and attempts to investigate the locations of adsorbates; if the surface is probed at high biases unintentionally one would make an erroneous attribution. Also, it is important to use a low surface bias when observing the filled states, particularly when studying adsorbates; in some extreme cases we have observed a surface which mimics a perfect surface at -2 V, but shows many defects at -1 V. These defects might influence the sites of adsorption or the electronic characteristics. If the adsorbates only influence the π and π^* states, they might be even invisible at high biases.

ACKNOWLEDGMENTS

This work was supported by the Shigekawa Project of TARA, University of Tsukuba. The support of a Grant-in-Aid for Scientific Research from the Ministry of Education, Science and Culture of Japan is also acknowledged.

*Electronic address: hata@ims.tsukuba.ac.jp,
hidemi@ims.tsukuba.ac.jp

World Wide Web: <http://dora.ims.tsukuba.ac.jp>

¹R. J. Hamers, R. M. Tromp, and J. E. Demuth, Phys. Rev. B **34**, 5343 (1986).

²R. J. Hamers, Ph. Avouris, and F. Bozso, Phys. Rev. Lett. **59**,

2071 (1987).

³R. A. Wolkow, Phys. Rev. Lett. **68**, 2636 (1992).

⁴A. W. Munz, Ch. Ziegler, and W. Gopel, Phys. Rev. Lett. **74**, 2244 (1995).

⁵H. Shigekawa, K. Hata, K. Miyake, M. Ishida, and S. Ozawa, Phys. Rev. B **55**, 15 448 (1997).

- ⁶K. Hata, M. Ishida, K. Miyake, and H. Shigekawa, *Appl. Phys. Lett.* **73**, 40 (1998).
- ⁷J. H. G. Owen, D. R. Bowler, C. M. Goringe, K. Miki, and G. A. D. Broggs, *Surf. Sci.* **341**, L1042 (1995).
- ⁸Y. J. Chabal, S. B. Christmann, E. E. Chaban, and M. T. Yin, *J. Vac. Sci. Technol. A* **1**, 1241 (1983).
- ⁹R. Ramstad, G. Brocks, and P. J. Kelly, *Phys. Rev. B* **51**, 14 504 (1995).
- ¹⁰Y. Enta, S. Suzuki, and S. Kono, *Phys. Rev. Lett.* **65**, 2704 (1990).
- ¹¹L. S. O. Johansson, R. I. G. Uhrberg, P. Martensson, and G. V. Hansson, *Phys. Rev. B* **42**, 1305 (1990).
- ¹²K. Hata (unpublished).
- ¹³H. Kageshima and M. Tsukada, *Phys. Rev. B* **46**, 6928 (1992).
- ¹⁴H. Tochihara, T. Amakusa, and M. Iwatsuki, *Phys. Rev. B* **50**, 12 262 (1994).
- ¹⁵D. Badt, H. Wengelnik, and H. Neddermeyer, *J. Vac. Sci. Technol. B* **12**, 2015 (1994).
- ¹⁶A. R. Smith, F. K. Men, K.-J. Chao, and C. K. Shih, *J. Vac. Sci. Technol. B* **14**, 914 (1996).
- ¹⁷P. Kruger, A. Mazur, J. Pollmann, and G. Wolfgarten, *Phys. Rev. Lett.* **57**, 1468 (1986).
- ¹⁸P. Kruger and J. Pollmann, *Phys. Rev. B* **38**, 10 578 (1988).